Thin Solid Films 540 (2013) 112–117

Contents lists available at SciVerse ScienceDirect

Thin Solid Films

journal homepage: www.elsevier.com/locate/tsf

Composite oxygen-barrier coating on a polypropylene food container

Seong Jin Kim [a], Eunkyung Song [b], Kyoungsik Jo [b], Taekyung Yun [b], Myoung-Woon Moon [a,*], Kwang-Ryeol Lee [a]

[a] Institute for Multi-disciplinary Convergence of Matter, Korea Institute of Science and Technology, Seoul 130-791, Republic of Korea
[b] Packaging R&D Team, CJ Cheiljedang, Seoul 100-400, Republic of Korea

ARTICLE INFO

Article history:
Received 3 September 2012
Received in revised form 7 June 2013
Accepted 7 June 2013
Available online 14 June 2013

Keywords:
Barrier coating
Food container
OTR
SiO_x
HMDSO
Buckling delamination

ABSTRACT

The composite oxygen-barrier coating of plasma polymerized-hexamethyldisiloxane (pp-HMDSO) and silicon oxide (SiO_x) on polypropylene (PP) was performed to lower the oxygen transmission rate. A pp-HMDSO interlayer was employed to cover PP pores at a relatively high porosity and provide better a thermal and mechanical buffer between brittle SiO_x and soft and porous PP. There is an optimum thickness for the pp-HMDSO and SiO_x films due to competition between the accumulated strain energy by compression in the composite layers and the interfacial adhesion strength. By choosing the optimal thickness of the layers, the oxygen transmission rate was improved from 7.42×10^{-4} for a pristine PP container to 2.6×10^{-5} cm^3/m^2-day-Pa with 8 ± 2 nm pp-HMDSO and 24 ± 6 nm SiO_x layers.

1. Introduction

Plastic food containers have been used globally to replace conventional food container composed of metals, ceramics and papers due to their low price and high throughput in mass production [1]. However, the atomic scale porosity (or low density) of plastic containers is an important drawback because it easily transmits oxygen, which makes the food stale. To overcome this drawback, research on oxygen-barrier coatings has been performed widely with various methods, such as high-density layered materials or coating with high-density metals or inorganic materials [1]. Among the several plastic materials used for food containers, polyethylene terephthalate (PET) is well-known to be easily coated by a thin oxygen-barrier film due to its relatively low porosity and high surface energy (31 ~ 47 mN/m) [2–5]. Dense thin films, such as silicone oxide (SiO_x) or diamond-like carbon (DLC), have been deposited on plastic containers using plasma systems [2,3,6,7]. DLC-coated PET bottles showed satisfactory performance for commercialized beverage containers and other applications [8]. Polypropylene (PP) is known to be a major material for food packaging with extremely low costs, an inherent water vapor barrier, and thermal resistance [6]. The material, however, has high porosity and low surface energy (23 ~ 36 mN/m), which limit its application when a high oxygen barrier is required. Furthermore, the high porosity and the low surface energy are unfavorable for additional functional coatings for higher oxygen barriers due to the difficulties of covering pores and the weak interface adhesion between PP and coating layers [2,3,9–11]. The poor adhesion between PP and the coating layers causes interface cracking due to the high strain energy of the deposited film, and the film under compression delaminates from PP to release strain energy. Inagaki et al. [3] applied argon pre-treatment on PP to improve the interfacial adhesion strength and a buffer layer to fill pores by immersing of 40 μm-thick PP in a methanol solution of tetramethoxysilane. These researchers reported that the oxygen transmission rate (OTR) of pristine PP was reduced from 2.2×10^{-2} to 3.65×10^{-4} cm^3/m^2-day-Pa. The barrier improvement factor (BIF), which is the OTR of the pristine PP substrate divided by that of the coated substrate, was 60. However, the absolute OTR value is still higher than that of DLC-coated PET, which has an OTR of ~1.0×10^{-5} cm^3/m^2-day-Pa [12]. Körner et al. [6,7] reached a low OTR of 5.03×10^{-5} cm^3/m^2-day-Pa on 30-μm-thick PP with OTR of 3.06×10^{-2} cm^3/m^2-day-Pa and a high BIF of 608 by applying a SiO_x coating, which was fabricated by employing a discontinuous process of 4 s of plasma operation and 10 s of off-time. The discontinuous process was used to reduce the effect of the thermal expansion of PP, which would cause the oxygen-barrier film to crack.

In this study, we suggest that proper coating conditions should be chosen in terms of interfacial adhesion and optimal thickness of the coating layer for the optimal coating to lower the OTR because simply increasing in the coating thickness has been reported not to enhance the oxygen-barrier properties proportionally [3,6,7]. It is known that oxygen-barrier performance is enhanced with the increase in the thickness until the interfacial adhesion is sufficient to support the strain energy of the film adhered on the substrate. For a given interfacial adhesion strength, the deposited layer may delaminate from the

* Corresponding author. Tel.: +82 2 958 5487; fax: +82 2 958 5451.
E-mail address: mwmoon@kist.re.kr (M.-W. Moon).

0040-6090/$ – see front matter © 2013 Elsevier B.V. All rights reserved.
http://dx.doi.org/10.1016/j.tsf.2013.06.009

PP or fail as the thickness increases (the interfacial adhesion energy is exceeded by the strain energy, which is proportional to the thickness of the coating layer) [13]. Correspondingly, with an increase of the coating thickness, the oxygen-barrier performance decreases due to the mechanical failure of the coating layer. Thus, it can be considered that there is an optimum thickness of the coating layer to provide the food container with a high oxygen-barrier performance.

To identify the optimum thickness of the deposited layers, we deposited composite films consisting of plasma polymerized hexamethyldisiloxane (pp-HMDSO) and SiO_x on PP. We systematically tuned the thickness of pp-HMDSO and SiO_x. The stress and the coating instability were explored by stress measurements and scratch tests, respectively. Furthermore, instabilities, such as delamination, buckling and cracking of composited layers, were observed by scanning electron microscopy (SEM). The OTR was evaluated on bowl-shaped PP with and without coatings.

2. Experimental details

We prepared a rectangular PP bowl container with a height of 25 mm, lengths in the range of 65–96 mm, and a thickness of 0.55 mm, as shown in Fig. 1a. To produce uniform coatings, a bowl-shaped stainless steel mold was designed following the outer geometry of a PP bowl as shown in Fig. 1b. Next, the stainless steel mold containing a PP bowl was placed on the cathode in the radio frequency-chemical vapor deposition chamber. The chamber is cylindrical in shape with a diameter of 270 mm and a height of 190 mm. After vacuuming the chamber to 0.13 Pa, oxygen pre-treatment with a flow rate of 20 sccm was performed for 1 min to enhance the adhesion on PP. A short duration of oxygen-plasma treatment was chosen because plasma treatment for longer than 1 min is known to produce a nano-porous structure on PP due to heterogeneous etching, which would act as defect sites for the cracking of the deposited layers [14]. Next, a pp-HMDSO interlayer was coated on the oxygen plasma-treated PP using a precursor of HMDSO vapor with a flow rate of 2 sccm. Finally, a SiO_x thin film was deposited on the pp-HMDSO interlayer using a mixture precursor of HMDSO vapor and oxygen gas with the flow rate ratio of HMDSO vapor over oxygen gas of 1/20 sccm/sccm. A schematic of a composite coating of pp-HMDSO/SiO_x is depicted in Fig. 1c. All plasma processes were conducted at a working pressure of 1.3 Pa and a bias voltage of −400 V. The deposition process is summarized in Table 1.

The deposition rates of pp-HMDSO and SiO_x were measured using an atomic force microscope (AFM, XE-70, Park Systems Corp.). The measurement was performed in a non-contact mode using the probe (ppp-NCHR, Nanosensors) with a tip radius of curvature of less than 10 nm. And the surfaces were observed using the SEM (NanoSEM, FEI Company) with the accelerating voltage at 10 kV. An X-ray photoelectron spectroscopy system (XPS, XPS System, ulvac-PHI) was used to characterize the chemical composition of the coated SiO_x films with respect to the flow rate ratio. For the XPS analysis, 100 nm-thick SiO_x films were deposited on a Si wafer. Before analyzing each film, it was cleaned by the argon ion beam etching with the accelerating voltage of 3 kV for 30 s. Then, an Al Kα (1486.6 eV) X-ray source was used as the excitation source, and the anode was maintained at 25 W and 15 kV at a chamber in the working pressure of 1.0×10^{-7} Pa with a beam spot size of 100 μm × 100 μm. The residual stresses of SiO_x and pp-HMDSO films were measured by a stress tester (JLCST022, J&L Tech) by varying thicknesses up to 55 nm on Si and PP thin strips with an area of 3 mm × 60 mm and thicknesses of 110 and 180 μm, respectively. The elastic modulus of Si and PP strip were 170 and 1.7 GPa respectively. Here, PP's elastic modulus was measured by a universal testing machine (UTM, Instron 5543, Instron). A scratch test was conducted using a scratch tester (JLST022, J&L tech) to test the coating failure of the oxygen-barrier coating on PP. A fine diamond tip of radius 200 μm was used for scratching. The normal load was increased uniformly from 0 to 10 N at a scratching speed of 0.1 mm/s for a distance of 2 mm. The experiment was repeated three times on the samples. The scratched path was later observed by SEM.

The performance of the oxygen-barrier was evaluated using OTR data, which were measured according to ASTM standard method F 1307 by a permeation test system (OX-TRAN 2/61, Mocon Inc.). For the measurement, the whole body of PP bowl was used by bonding the top surface of the PP bowl in Fig. 1a to the measurement unit. Next, the oxygen inside the bowl was degased with the introducing N_2 gas at a rate of 10 cm^3/min for more than 1 day. The samples were subsequently exposed to 50% relative humidity of the air (21% O_2) at a temperature of 23 °C (±2 °C) and a pressure of 1.01×10^5 Pa outside of the bowl. After waiting more than 1 day for the OTR to reach its steady value, the OTR was measured for 1 day. At least two samples for each data were tested to check the repeatability.

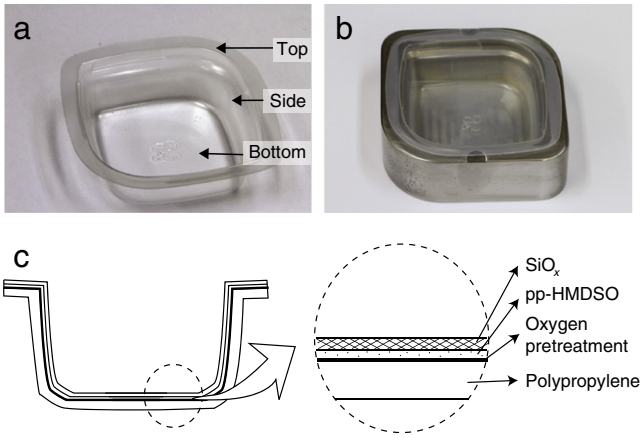

Fig. 1. (a) Polypropylene (PP) food container with a bowl shape and (b) a stainless steel mold filled with a PP bowl. (c) A schematic of a composite coating of pp-HMDSO/SiO_x on a PP bowl pre-treated by oxygen plasma.

3. Results and discussion

3.1. Characterization of the composite layers

For an oxygen barrier coating on PP, a coating of SiO_x film, which is known to have good oxygen-barrier properties, was used with different chemical compositions by changing the flow rate ratio of the HMDSO vapor and the O_2 gas mixture. The SiO_x film formed from a precursor mixture of HMDSO vapor and oxygen gas with a sufficiently low HMDSO/O_2 flow rate ratio (<1/5) is known to be almost carbon-free because oxygen ions restrict the deposition of carbon ions by forming CO_2 during the deposition process [6,7]. Three types of SiO_x films were prepared with different flow rate ratios (HMDSO vapor/oxygen gas) of 2/20, 1/20 and 0.5/20 sccm/sccm for chemical analysis using XPS. As a reference, a pure pp-HMDSO film produced with a HMDSO flow rate of 2 sccm was analyzed, as well. The relative chemical compositions between the elements of Si, O and C indicated that

Table 1
Summary of the deposition process of a composite oxygen-barrier film (pp-HMDSO/SiO_x).

Process	Precursor gases	Bias voltage (-V)	Working pressure (Pa)
Pretreatment	O_2	400	1.3
Deposition of interlayer (pp-HMDSO)	HMDSO vapor		
Deposition of oxygen-barrier film (SiO_x)	HMDSO vapor & O_2		

less carbon existed in the SiO_x films as more oxygen gas was injected, as listed in Table 2. Previous research revealed that good oxygen-barrier properties appeared when the SiO_x film formed by a mixture of HMDSO vapor and oxygen gas contained less carbon than $SiO_{1.9}C_{0.2}$, which confirms that our conditions for SiO_x are suitable for the formation of good oxygen-barriers [7].

Although a stainless steel mold was used to provide the uniformity of the coating thickness, the non-uniformity of the coating thickness between the bottom and the tilted side was still observed. The difference in the deposition rate could be explained by the difference in the amount of reflected ions or non-deposited ions during plasma process, depending on the incidence angle of ions on the substrate [15]. Thus, the average deposition rate on the bottom was 1.5 ± 0.16 times higher than that on the tilted side, even though we tried to minimize such non-uniformity using a stainless steel mold. To indicate this effect in the graph, we introduced the error bar for the coating thickness in Figs. 3 and 6.

The residual stress was estimated from the observed curvature of the film/substrate using a laser reflection method and the Stoney equation written as $\sigma \approx -E_s h_s^2/(h_f R)$ [16], where σ is the residual stress of film [N/m^2], E_s is the elastic modulus of substrate [N/m^2], h_s and h_f are the thickness [m] of substrate and film, respectively, and R is the radius [m] of curvature of the film/substrate. Both residual stresses of pp-HMDSO and SiO_x are found to be significantly affected by the variation of the coating thickness on Si strip as shown in Fig. 2. On Si strip, both compressive stresses increased with lowering the coating thickness. However, when pp-HMDSO was deposited onto PP strip, the residual stress rather remained at a constant value of -0.14 ± 0.077 GPa on the average, regardless of the coating thickness. These stress values on Si and PP strips are found to be similar with previous results [7,17].

3.2. Oxygen-barrier performance and crack analysis

The oxygen-barrier performance of the SiO_x film fabricated with the flow rate ratio of 1/20 sccm/sccm for HMDSO/O_2 was investigated with and without the buffer-layer of pp-HMDSO. The OTR for a 24 ± 6 nm SiO_x film deposited onto oxygen plasma-treated PP was evaluated to be 3.3×10^{-4} cm^3/m^2-day-Pa, which is lower than the value of 7.42×10^{-4} cm^3/m^2-day-Pa for pristine PP, as shown in Fig. 3a. However, there was no significant improvement in the OTR with increasing thickness of SiO_x up to 80 ± 20 nm (OTR = 2.9×10^{-4} cm^3/m^2-day-Pa), which is also comparable to the result with 1 min of O_2 plasma-treatment on the PP reducing the OTR to 3.2×10^{-4} cm^3/m^2-day-Pa. The OTR improvement by O_2 plasma is known to be caused by the surface rearrangement of the PP which was studied by J.F. Friedrich, et al. using the permeation test for *n*-pentane [18]. The low barrier performance with SiO_x film can be explained by the high porosity of PP, which would not be covered by fine molecules of SiO_x, and the crack formation in the coated film on the PP surfaces due to low interfacial strength against high compression in the film. However, when the pp-HMDSO interlayer was used between the PP and the SiO_x, the oxygen-barrier performance was enhanced significantly in comparison to that of the pristine PP, as shown in Fig. 3b. In addition, during the plasma of the mixture gases of HMDSO/O_2 for producing a SiO_x coating on the PP, the large portion of oxygen plasma has a chance to cause the heterogeneous etching on the PP [14]. The SEM images in Figs. 3c-d indicate the increase of the surface roughness for the SiO_x (24 ± 6 nm) coated PP formed by the undesired heterogeneous etching. Such roughness would inhibit the PP with high porosity from being uniformly covered by the barrier coating. However, when the pp-HMDSO interlayer was used between the PP and the SiO_x, the oxygen-barrier performance was significantly enhanced in comparison to that of the pristine PP as shown in Fig. 3b. It is known that pp-HMDSO plasma provides a coating layer on PP without undesired heterogeneous etching [19]. Furthermore, pp-HMDSO would cover the large pores of PP due to the relatively coarse and flexible nature by comparison to dense oxygen-barrier coating materials, such as SiO_x and DLC [7,20]. Additionally, when there are mechanical and thermal impacts on SiO_x from external sources such as mechanical scratches or heating, pp-HMDSO is known to protect the SiO_x film by relieving the stress through its flexible properties [7]. It was found that the OTR decreased with an increase of the thickness of pp-HMDSO up to 8 ± 2 nm, while the OTR value increased with an increase of the thickness over 8 ± 2 nm, which indicates there is an optimum condition for the lowest OTR with respect to the coating thickness. This behavior of the OTR value was correlated with surface instabilities investigated by SEM, as presented in Figs. 3e–f. Clear surface was observed for relatively thin films of pp-HMDSO (8 ± 2 nm)/SiO_x (24 ± 6 nm) in Fig. 3e, while severe cracks on the film with thicker pp-HMDSO thickness (40 ± 10 nm)/SiO_x (24 ± 6 nm) as shown in Fig. 3f.

We further investigated the surface failures of buckling delamination and further cracking of coating layers to understand the origin of the crack evolution of the films deposited on PP. To reveal the failures, we prepared PP with pp-HMDSO (40 ± 10 nm)/SiO_x (24 ± 6 nm) for a surface with a higher density of cracks. Fig. 4 shows the delamination of a composited layer with a telephone cord shape, which was induced by relatively high compressive strain energy and low adhesion strength. Ridge cracking was also observed on the delaminated surface, as shown in Fig. 4. Such ridge cracking has been known to possibly evolve only when the coating material is brittle, and buckling delamination occurs during the stress relaxation process of the compressed coating [21]. Such patterns of compressed thin films are known to be easily formed on defect sites [13,22], which indicates that the accumulated strain energy induced by the thickness and the compressive stress of pp-HMDSO (40 ± 10 nm)/SiO_x (24 ± 6 nm) is much higher than the interfacial adhesion strength. The stresses in compression of SiO_x are high, greater than ~0.1 GPa, while the adhesion on PP is well-known to be quite low due to its low surface energy. These interface delamination and film buckling failures act as defects to leak gases. Many previous researchers have already indicated these defects as the most crucial origin for the

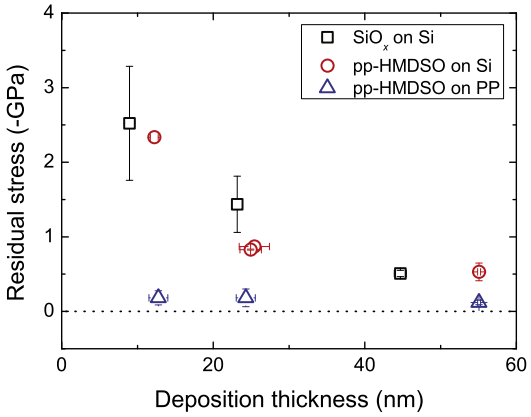

Fig. 2. Plot of the residual stress of pp-HMDSO and SiO_x deposited onto Si and PP strip versus the coating thickness.

Table 2
XPS result for the SiO_x film deposited with different flow rate ratios of HMDSO vapor and oxygen gas.

Flow rate ratio of HMDSO/O_2 [sccm/sccm]	2/20	1/20	0.5/20
Chemical composition of Si:O:C[%]	31.3:66.4:2.3	31.2:66.9:1.9	31.2:67.5:1.3

* Pure pp-HMDSO film has the chemical composition of Si:O:C = 19.8:29.1:51.1.

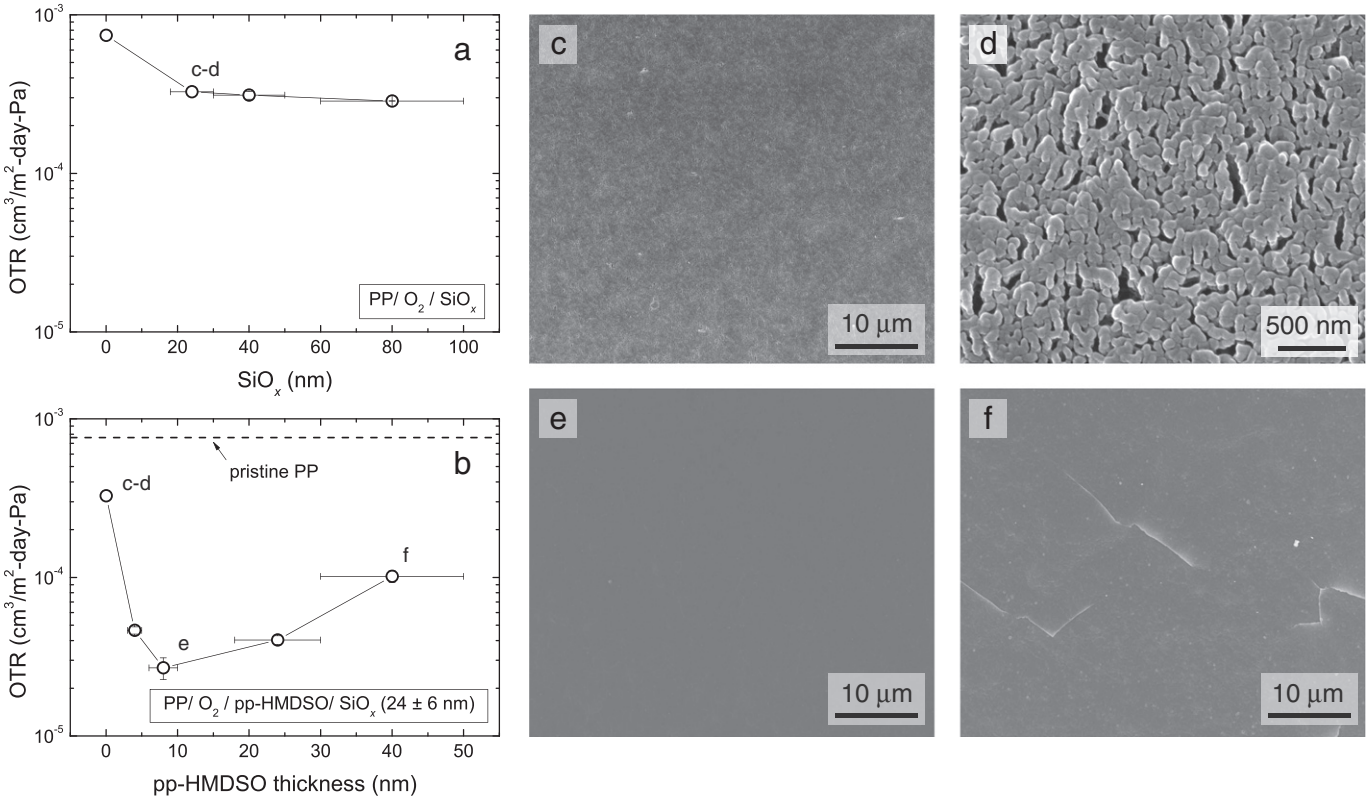

Fig. 3. Semi-log graph of the OTR versus the thickness of (a) SiO_x in a single layer coating of $PP/O_2/SiO_x$ and (b) pp-HMDSO in a composite coating of PP/O_2/pp-HMDSO/SiO_x (24 ± 6 nm). SEM images captured on the tilted side of specimens of (b) with a pp-HMDSO thickness of (c-d) 0, (e) 8 ± 2 and (f) 40 ± 10 nm.

fatal deterioration of the oxygen-barrier performance [6,23–25]. These defects are believed to evolve as a point defect in the micron and submicron range and to be further extended to defects such as cracks [23]. Accordingly, the high permeability of the PP substrate further deteriorates the oxygen-barrier performance compared to that of the PET substrate [26]. The PP substrate is known to have approximately 10 times higher oxygen permeability than PET in the same experimental conditions due to the inherently high porosity of PP [27].

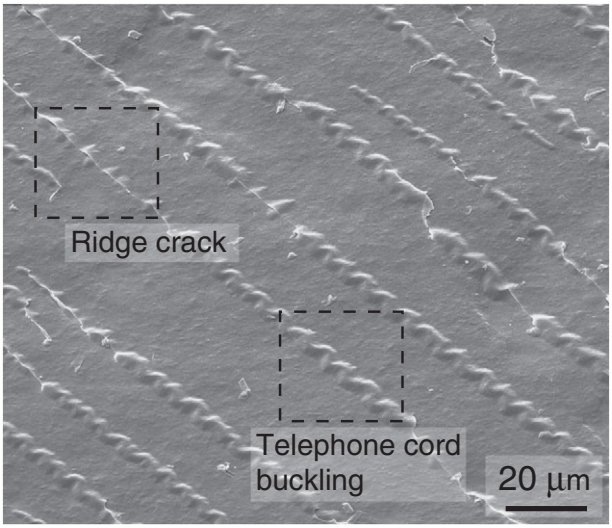

Fig. 4. SEM images of the delamination in the shape of a telephone cord and a ridge-crack on a buckled film on the oxygen-barrier coating with pp-HMDSO (40 ± 10 nm)/SiO_x (24 ± 6 nm).

Overall, it can be concluded that the cracking of the composite layer would decrease the OTR value for thicker coatings on PP.

We further investigated the stability of the deposited layers by performing scratching tests. Fig. 5 shows a scratch track on the oxygen-barrier coating with pp-HMDSO (8 ± 2 nm)/SiO_x (24 ± 6 nm), which has a non-cracked surface observed in the SEM view of Fig. 3e. However, after passing the scratch position of 0.5 mm (here, the corresponding normal force is 1.7 N) from the starting origin, a buckled crack induced from interfacial failure evolved on the surface as shown in Figs. 5a–c. And to elucidate the influence of the film thickness, we further performed scratch tests on pp-HMDSO/SiO_x (24 ± 6 nm) layers with a variation of pp-HMDSO thicknesses from 5 to 20 nm as shown in Fig. 5d. As increased the film thickness, cracking was observed on the samples for lower normal force. For the sample with higher thickness, the accumulated strain energy by the external force exceeds the adhesion strength at the interface between film and substrate. The result suggested that the coating thickness of the deposited layer on PP within the critical value not to exceed the given interfacial adhesion level is an important factor because delamination and further cracking may be caused by a high strain energy accumulated with an increase of the film thickness. Given the importance of coating thickness, the OTR was measured by changing the thicknesses of SiO_x and pp-HMDSO, as shown in Fig. 6. The black line in Fig. 6 is the OTR value for a pure pp-HMDSO film with different thicknesses on PPs without a SiO_x coating, showing no significant enhancement of the oxygen-barrier performance due to the lower density of pp-HMDSO [20]. However, for composite coatings of pp-HMDSO/SiO_x, the OTR value decreased drastically. It was revealed that the optimum thickness of SiO_x is 24 ± 6 nm for the optimum OTR. It was also found that increasing the SiO_x thickness over a specific thickness (24 ± 6 nm) causes a degradation of the oxygen-barrier performance, which agrees with the previous argument that there is

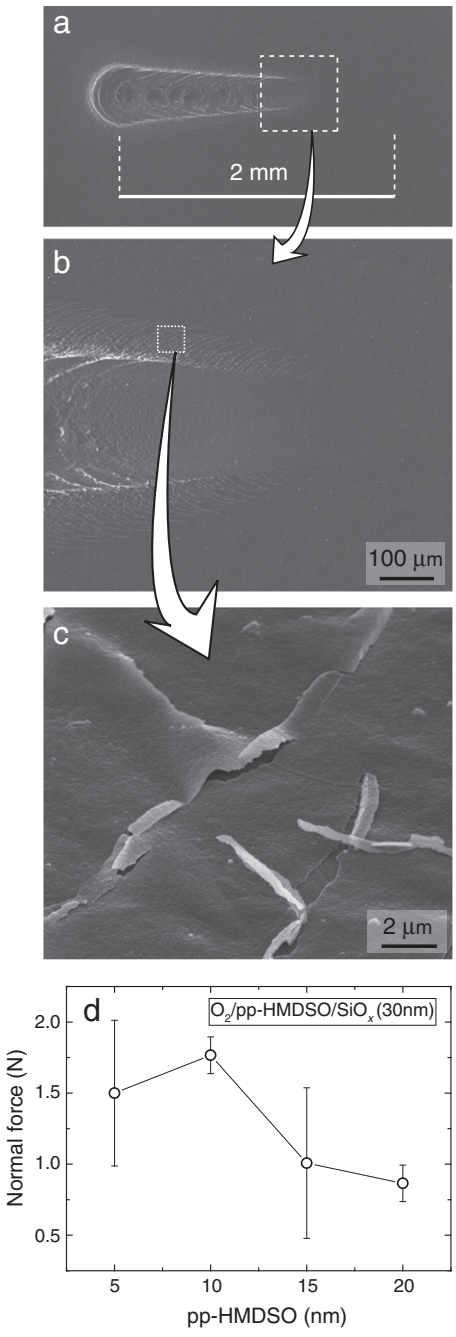

Fig. 5. SEM images of (a) a scratch track on the oxygen-barrier coating with pp-HMDSO (8 ± 2 nm)/SiO_x (24 ± 6 nm), (b) a magnified image of the area indicated in (a), clearly showing the initiation of cracking, and (c) the magnified image marked in (b), showing the crack shape observed at an oblique angle of 40 degrees. (d) Plot of the onset normal force causing the crack on the coating film versus the pp-HMDSO thickness.

an optimum thickness of pp-HMDSO by considering the accumulated strain energy of the film competing with the interfacial adhesion strength. At this optimum thickness of pp-HMDSO (8 ± 2 nm) and SiO_x (24 ± 6 nm), the OTR decreased from 7.42 × 10^{-4} for a pristine PP container to 2.6 × 10^{-5} cm^3/m^2-day-Pa with a BIF of 29. For this optimum thickness, the total coating thickness was measured to be 40 nm at the bottom of the PP bowl, while the side wall was 24 nm. Even if our coating has a non-uniform coating thickness due to the 3D bowl shape, the achieved OTR of 2.6 × 10^{-5} cm^3/m^2-day-Pa is a remarkably good result compared with a commercialized PET bottle with an OTR ~ 1 cm^3/m^2-day-Pa [3,7,8]. In optimum condition, the side wall thickness is still within the critical value for good barrier

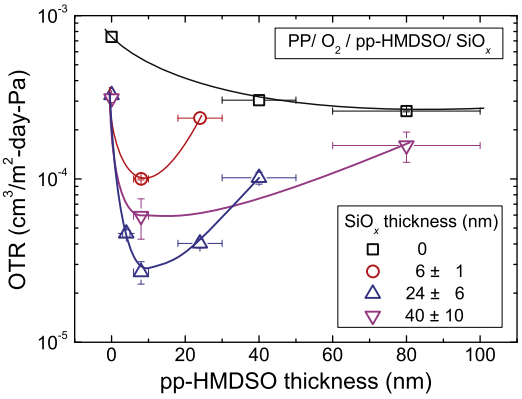

Fig. 6. A semi-log graph of the OTR versus the thickness of pp-HMDSO for various SiO_x thicknesses in composite films of PP/O_2/pp-HMDSO/SiO_x.

performance while the coating film remains free from cracks [6,23,24]. Next, at this optimized thickness composition, we further tested the effect of the HMDSO/O_2 flow rate ratio and the bias voltage on the oxygen barrier performance. The HMDSO/O_2 flow rate ratio was tuned from 1/20 to 4/20 sccm/sccm at a bias voltage of −400 V, and the bias voltage was tuned from −500 to −300 V at a HMDSO/O_2 ratio of 1/20 sccm/sccm. A clear dependency of the HMDSO/O_2 flow rate ratio and the bias voltage on the OTR was observed. The film becomes more carbon-free (or more similar to silicon dioxide) with a decreasing HMDSO/O_2 ratio, indicated in Table 2, while the OTR clearly decreases as shown in Fig. 7a. When the bias voltage is tuned from −500 to −300 V, the bias voltage of −400 V was found to provide the best OTR as shown in Fig. 7b. At high bias voltage of −500 V a denser coating forms with higher plasma energy [19]. A

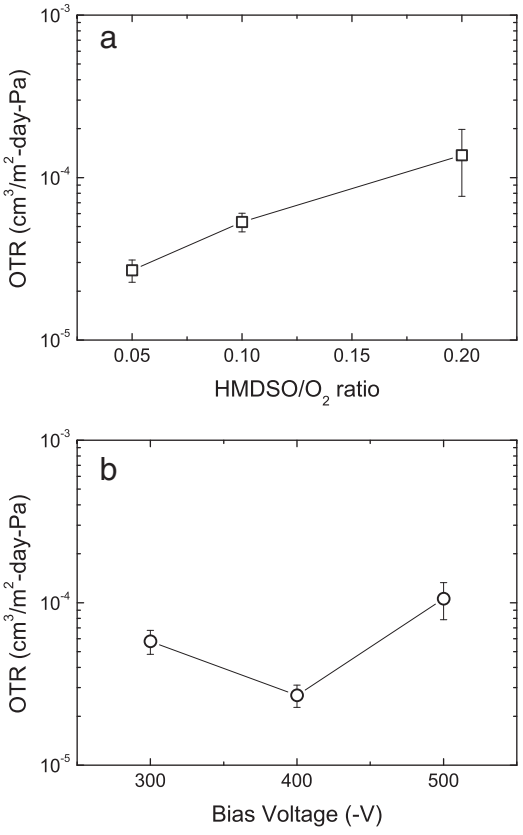

Fig. 7. A semi-log graph of the OTR versus (a) the HMDSO/O_2 flow rate ratio and (b) the bias voltage for the coating of pp-HMDSO (8 ± 2 nm)/SiO_x (24 ± 6 nm).

denser film could have a better barrier performance, but it could also be easily cracked due to the increased strain energy.

Conclusions

The oxygen-barrier properties were investigated for a composite coating of pp-HMDSO/SiO_x on bowl-shaped PP food containers. When a single-layer coating of SiO_x was applied to the PP food container, there was a clear limitation in the enhancement of the oxygen-barrier property. However, when a pp-HMDSO interlayer was inserted as a buffer layer between the SiO_x and PP, the OTR was significantly decreased compared to that of the SiO_x film without pp-HMDSO. The pp-HMDSO interlayer would cover the large pores of PP due to the relatively coarse and flexible nature as well as inhibit surface roughening during a SiO_x coating process. It was found that there is an optimum thickness for pp-HMDSO and SiO_x because a thicker coating of the composite layer than the optimum thickness caused severe coating instabilities, which would degrade the OTR. The optimum thicknesses of pp-HMDSO and SiO_x were found to be 8 ± 2 and 24 ± 6 nm, respectively. With these thicknesses, the OTR was improved from to 7.42×10^{-4} cm^3/m^2-day-Pa for a pristine PP container to 2.6×10^{-5} cm^3/m^2-day-Pa for PP with a composite coating. Thus, it can be concluded that it is important to deposit oxygen-barrier coatings with composite layers at an optimal thickness.

Acknowledgments

This work was supported by CJ Cheiljedang and the KIST internal project (2E23920).

References

[1] A. Arora, G.W. Padua, J. Food Sci. 75 (2010) R43.
[2] D.S. Finch, J. Franks, N.X. Randall, A. Barnetson, J. Crouch, A.C. Evans, B. Ralph, Packag. Technol. Sci. 9 (2) (1996) 73.
[3] N. Inagaki, S. Tasaka, T. Nakajima, J. Appl. Polym. Sci. 78 (13) (2000) 2389.
[4] J.R. Dann, J. Coll. Interface Sci. 32 (1970) 302.
[5] D.K. Owens, R.C. Wendt, J. App. Polym. Sci. 13 (1969) 1741.
[6] L. Körner, A. Sonnenfeld, Ph. Rudolf von Rohr, Thin Solid Films 518 (17) (2010) 4840.
[7] L. Körner, A. Sonnenfeld, R. Heuberger, J.H. Waller, Y. Leterrier, J.A.E. Månson, Ph. Rudolf von Rohr, J. Phys. D: Appl. Phys. 43 (2010) 115301.
[8] A. Shirakura, M. Nakaya, Y. Koga, H. Kodama, T. Hasebe, T. Suzuki, Thin Solid Films 494 (2006) 84.
[9] J.H. Sewell, Mod. Plasts. 48 (6) (1971) 66.
[10] C. Bonnerup, P. Gatenholm, J. Adhsn. Sci. Tech. 7 (1993) 247.
[11] A.P. Roberts, B.M. Henry, A.P. Sutton, C.R.M. Grovenor, G.A.D. Briggs, T. Miyamoto, M. Kano, Y. Tsukahara, M. Yanaka, J. Membrane Sci. 208 (2002) 75.
[12] Y. Ohsone, H. Nishi, M. Saito, M. Suzuki, H. Murakami, N. Ohtake, J. Solid Mech. Mater. Eng. 3 (2009) 691.
[13] M.-W. Moon, K.-R. Lee, K.H. Oh, J.W. Hutchinson, Acta Mater. 52 (2004) 3151.
[14] C.H. Wanke, J.L. Feijó, L.G. Barbosa, L.F. Campo, R.V.B. de Oliveira, F. Horowitz, Polymer 52 (8) (2011) 1797.
[15] M. Joe, M.-W. Moon, J. Oh, K.-H. Lee, K.-R. Lee, Carbon 50 (2012) 404.
[16] G.G. Stoney, Proc Roy Soc London A 82 (1909) 172.
[17] Y. Rahmawan, K.-J. Jang, M.-W. Moon, K.-S. Kim, K.-R. Lee, K.-Y. Suh, Langmuir 26 (1) (2010) 484.
[18] J.F. Friedrich, L. Wigan, W. Unger, A. Lippitz, J. Erdmann, H.-V. Gorsler, D. Prescher, H. Wittrich, Surf. Coat. Tech. 74–75 (1995) 910.
[19] L. Han, P. Mandlik, J. Gartside, S. Wagner, J.A. Silvernail, R.-Q. Ma, M. Hack, J.J. Brown, J. Electrochem. Soc. 156 (2009) H106.
[20] L. Agres, Y. Ségui, R. Delsol, P. Raynaud, J. Appl. Polym. Sci. 61 (11) (1996) 2015.
[21] S. Faulhaber, C. Mercer, M.-W. Moon, J.W. Hutchinson, A.G. Evans, J. Mech. Phys. Solids 54 (2006) 1004.
[22] M.-W. Moon, H.M. Jensen, J.W. Hutchinson, K.H. Oh, A.G. Evans, J. Mech. Phys. Solids 50 (2002) 2355.
[23] A.S. da Silva Sobrinho, G. Czeremuszkin, M. Latrèche, G. Dennler, M.R. Wertheimer, Surf. Coat. Technol. 116–119 (1999) 1204.
[24] H. Chatham, Surf. Coat. Technol. 78 (1996) 1.
[25] A.S. Da Silva Sobrinho, M. Latréche, G. Czeremuszkin, J.E. Klemberg-Sapieha, M.R. Wertheimer, J. Vac. Sci. Technol. A 16 (1998) 3190.
[26] A. Grüniger, Ph. Rudolf von Rohr, Thin Solid Films 459 (2004) 308.
[27] W. Andrew, Permeability and other film properties of plastics and elastomers, Plastics Design Library, New York. Norwich , 1995.